

Article

Comparative Study of the Structural and Electrical Properties of Nanoscale Calcium Ferrite Synthesized via Sol-Gel Auto-Combustion and Co-Precipitation Methods

Ghazwa Qahtan Ali*¹, Sabah Mohammed Ali²

1,2. Department of Physics, College of Education for Pure Sciences, University of Kirkuk, Kirkuk, Iraq

* Correspondence: ephm23006@uokirkuk.edu.iq

Abstract: Calcium ferrite ($CaFe_2O_4$) nanoparticles were synthesized using sol-gel auto-combustion and co-precipitation methods to investigate the influence of synthesis technique on structural, magnetic, morphological, and electrical properties. X-ray diffraction confirmed orthorhombic crystal structures in both methods, with enhanced crystallinity observed in sol-gel samples. VSM analysis revealed higher saturation magnetization in sol-gel products, while FE-SEM images showed more uniform particle morphology and reduced agglomeration. FTIR spectra confirmed efficient organic decomposition in sol-gel samples. Additionally, sol-gel-derived nanoparticles exhibited superior dielectric constants and AC conductivity. Overall, the sol-gel method offered better control over phase purity, magnetic strength, and electrical behavior, making it more suitable for advanced applications, while the co-precipitation method remained effective for simpler, cost-efficient synthesis.

Keywords: Calcium Ferrite, ($CaFe_2O_4$), Sol-Gel Auto-Combustion, Co-Precipitation, XRD, VSM, FE-SEM, FTIR, Dielectric Properties, Nanomaterials

Citation: Ali, G. Q., Ali, S. M. Comparative Study of the Structural and Electrical Properties of Nanoscale Calcium Ferrite Synthesized via Sol-Gel Auto-Combustion and Co-Precipitation Methods. Central Asian Journal of Medical and Natural Science 2025, 6(3), 1356-1367.

Received: 24th May 2025

Revised: 31st May 2025

Accepted: 03rd Jun 2025

Published: 24th Jun 2025



Copyright: © 2025 by the authors. Submitted for open access publication under the terms and conditions of the Creative Commons Attribution (CC BY) license (<https://creativecommons.org/licenses/by/4.0/>)

1. Introduction

Spinel ferrites possess distinctive structural and magnetic properties, making them a focus of researchers in recent years. Its chemical stability, abundance in nature, high saturation magnetization, and high electrical resistance make it a suitable material as power transformers [1], for use in electronic and communications applications. Since the structural magnetic nanoparticles are primarily utilized in a variety of fields, including magnetic fluids [2], catalysis [3], and biomedical applications [4].

The magnetic characteristics of these metal nanoparticles are influenced by their shape and size [5]. Currently, magnetic oxide nanoparticles are particularly intriguing and hold considerable interest due to their extensive applications, spanning from fundamental research to industrial settings [6]. Among the various types of nanoparticles, $CaFe_2O_4$ nanoparticles are attracting significant attention because of their remarkable catalytic, optical, and magnetic properties [7], [8]. Compared to other ferrites like $MnFe_2O_4$, $NiFe_2O_4$, $ZnFe_2O_4$, $CoFe_2O_4$, and $CuFe_2O_4$, calcium ferrite stands out for its biocompatibility and environmental friendliness, attributed to the presence of Ca^{2+} ions instead of heavy metals [9].

In addition to chemical stability and biocompatibility, these nanoparticles exhibit features that make them suitable for a wide range of applications [10]. Calcium and iron-

based compounds have been investigated for potential use in optical memory devices, while previous studies have explored their roles in steel production processes such as deoxidization, desulfuration, and dephosphorization, as well as in high-temperature sensors, gas absorption, and oxidation[11], catalysis. These attributes position CaFe_2O_4 nanoparticles as promising candidates for drug delivery systems. For effective drug delivery[12][13], magnetic nanoparticles must possess characteristics such as monodispersed, stability, superparamagnetic, and biocompatibility[14], with sizes that can be controlled within a few nanometers to tens of nanometers[15][16]. Various synthesis methods for magnetic nanoparticles include sol-gel, hydrothermal [17], co-precipitation[18], auto combustion[19], and aerosolization techniques[20]. Ferrites have been widely used as permanent magnets due to their excellent chemical stability, low production cost, and acceptable magnetic performance[21].

2. Materials and Methods

Materials

Calcium nitrate (99.9%), ferric nitrate (98%), citric acid (99.45%), and ethylene glycol (%99) were supplied from Qualikems, sodium hydroxide (99.5%) from Merck and absolute ethanol (99%) from LOBA Chemie. These chemicals were utilized in the synthesis of the samples used with distilled water.

Sample preparation methods

Co-precipitation

In this method, iron nitrate 80.8g and calcium nitrate 23.69g were added to 150ml of distilled water and continuously mixed in a magnetic stirrer until they were dissolved and homogenized at room temperature and then we added 6ml of ethylene glycol ethylene glycol and then we added sodium hydroxide solution (NaOH) with a concentration of 40% ,70ml until we obtained a pH value of 8-11, then we continuously mixed the mixture for two hours and then we used a centrifuge (3000 rpm center fugal) for 10 minutes for three times using distilled water and then dried in an oven at 90C and then we crushed the powder that we obtained and then we calcined the powder in an oven at different temperatures for three hours (500-700-900-1100)., resulting in calcium ferrite nanoparticles in powder form. The co-precipitation process is illustrated in Figure 1

Auto-combustion

In this method, 57.6gm of citric acid was dissolved in 20ml of distilled water and then 80.8gm of iron nitrate was dissolved in 30ml of distilled water, after which we dissolved 23.615gm of calcium nitrate in 20ml of distilled water separately in the magnetic stirrer and after dissolving each separately, these two solutions are mixed with the citric acid solution together over the magnetic stirrer and then the ammonia solution is added in drops until we get a pH equal to 7 and then mixing and then we start heating at a temperature of (80_85) degrees with mixing and continuing until we get (gel).Then we increase the temperature more and more until the temperature exceeds 200 degrees, and the combustion in this experiment was carried out at a temperature of 270c and calcium ferrite powder was obtained

Then the powder was calcined in an oven at temperatures (500-700-900-1100). After calcination, the sample was gently ground with a mortar and pestle, producing calcium ferrite nanoparticles in powdered form. The process is illustrated in Figure 1 (b).

Properties of CaFe_2O_4 NPs

The nanomaterials are synthesized in the required form and several tests are performed to characterize their properties, the most important of which are XRD, FTIR and SEM tests, which give important information about the size of the resulting crystals in addition to information about homogeneity, agglomeration and shape of the nanoparticles, and this procedure is necessary to test the effectiveness of ferrite in the

targeted applications, and the VSM test is necessary to measure the magnetic coefficients. The VSM test is necessary to measure the magnetic coefficients, through which the hydrogenation loop curve is produced, which gives information about the residual magnetism, saturation and coercive force of the ferrite, while characterization is done using the LCR meter to study the dielectric properties and deduce important constants such as dielectric constant, dielectric loss and dielectric loss tangent. The characterization processes are performed using different instruments that give spectra or images of the sample surface (mentioned above) of the prepared ferrite which is calcium ferrites, i.e. the same procedures are performed to study dielectric, magnetic or morphological properties.

3. Results and Discussion

XRD Tests

"When comparing the two preparation methods using X-ray diffraction examination, the sol-gel self-combustion method shows a gradual and clear crystallization progression with increasing sintering temperature, starting from an amorphous pattern (as-burnt), through the appearance of initial peaks at 700 °C, to almost complete and pure crystallization at 1100 °C with sharp peaks and good agreement with the ($CaFe_2 O_4$) standard (ICDD 00-0302-1068). The peaks were very sharp, and their number was large, indicating structural regularity and the presence of a pure rhombohedral phase without impurities. The crystal size (D_{sh}) increased with temperature up to 900 °C and then decreased at 1100 °C due to crystal rearrangement or partial disintegration, while the theoretical density remained almost constant"

"In contrast, the co-precipitation method shows relatively slow crystallization; the material starts in an amorphous state at as-burnt, and weak, blunt peaks appear at 500 °C indicating the onset of crystallization, but only gain sufficient clarity at 900 °C. At 1100 °C, there are sharp and distinct peaks indicative of high-quality crystallization and near-pure formation of the ($CaFe_2 O_4$) phase, but their intensity is slightly lower compared to the sol-gel route. This is because the interaction between the preparation components in co-precipitation is less homogeneous, and this may lead to localized variation in composition, The data show that the spontaneous combustion sol-gel method is more efficient in forming the pure crystalline phase over a wider range of temperatures, with higher structural regularity, while the co-precipitation method requires high temperatures to achieve similar crystallization", is shown in figure 1.

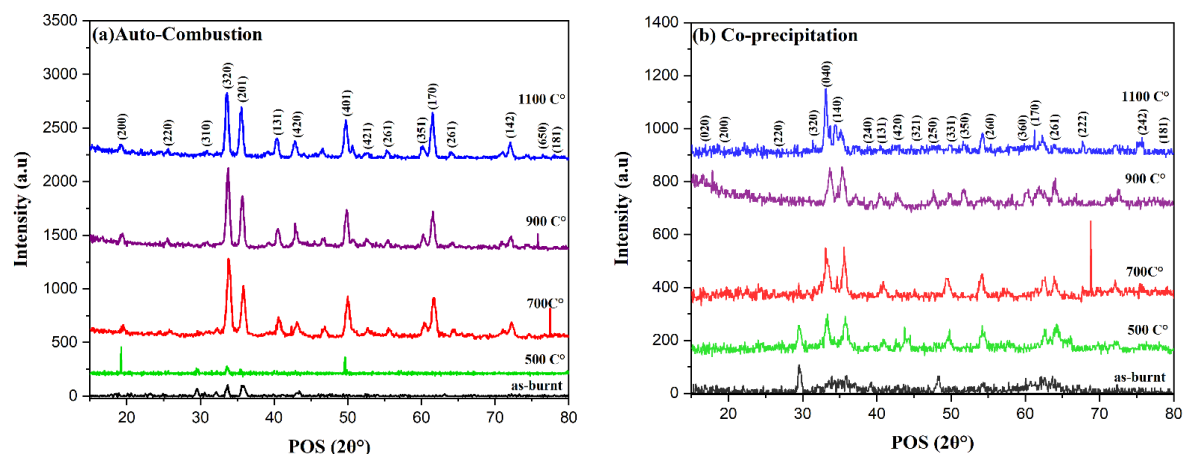
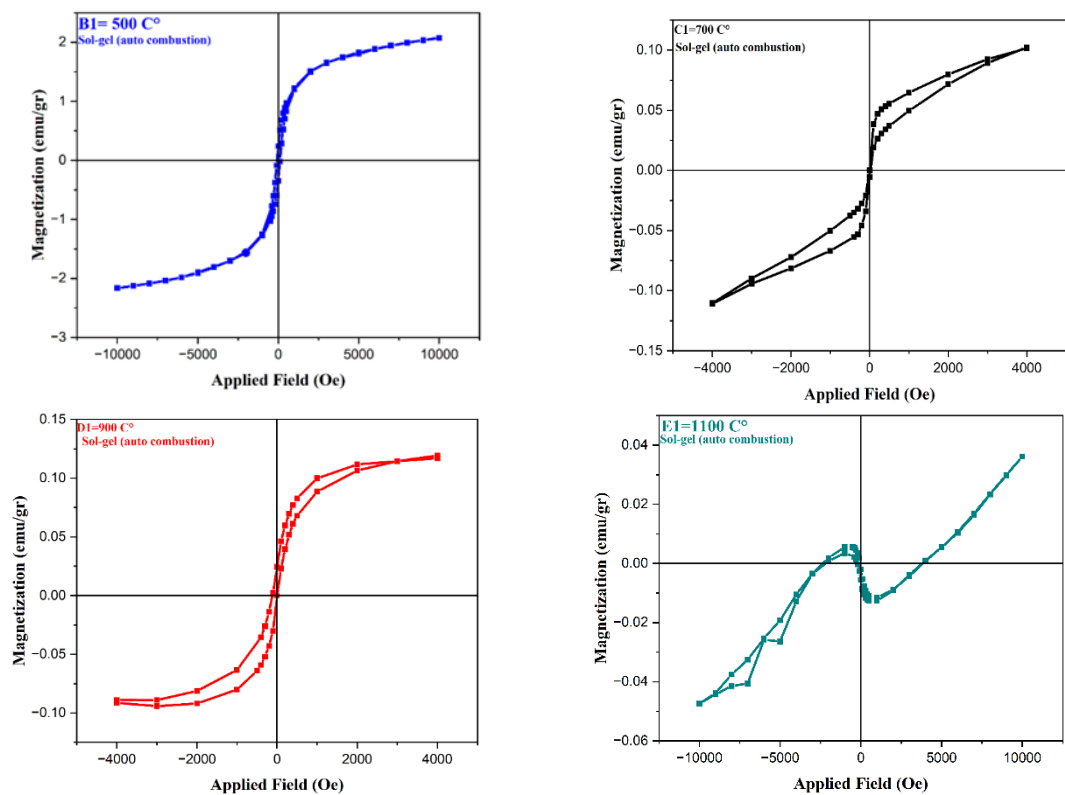


Figure 1. (a) X-ray diffraction (a) Auto - combustion (b) Co - precipitation.

VSM Tests

The magnetic results showed significant variation between the two methods. The spontaneous combustion sol-gel method recorded the highest saturated magnetism ($M_s \approx 2.08$ emu/g) at 500 °C, with a residual magnetization value $H_c \approx 75$ Oe, reflecting a clear ferromagnetic behavior due to the small grain size and uniform nanoparticle dispersion. At 900 °C, the properties decreased slightly, and at 1100 °C quasi-paramagnetic properties appeared due to agglomeration or excessive grain growth. In contrast, the co-precipitation method showed relatively weaker magnetic behavior at most temperatures. At 500 °C, M_s recorded ≈ 1.62 emu/g, a value lower than that of sol-gel. At higher temperatures, M_s continued to decrease, and features indicative of the formation of non-magnetic phases or internal structural disturbances appeared. The poor magnetic response is attributed to inhomogeneous grain growth and crystal anisotropy. Overall, the sol-gel method shows a higher ability to induce effective magnetic properties at low temperatures, making it suitable for sensitive magnetic applications, unlike co-precipitation, which requires special thermal conditions to achieve similar performance.

VSM Test (a) Auto - Combustion



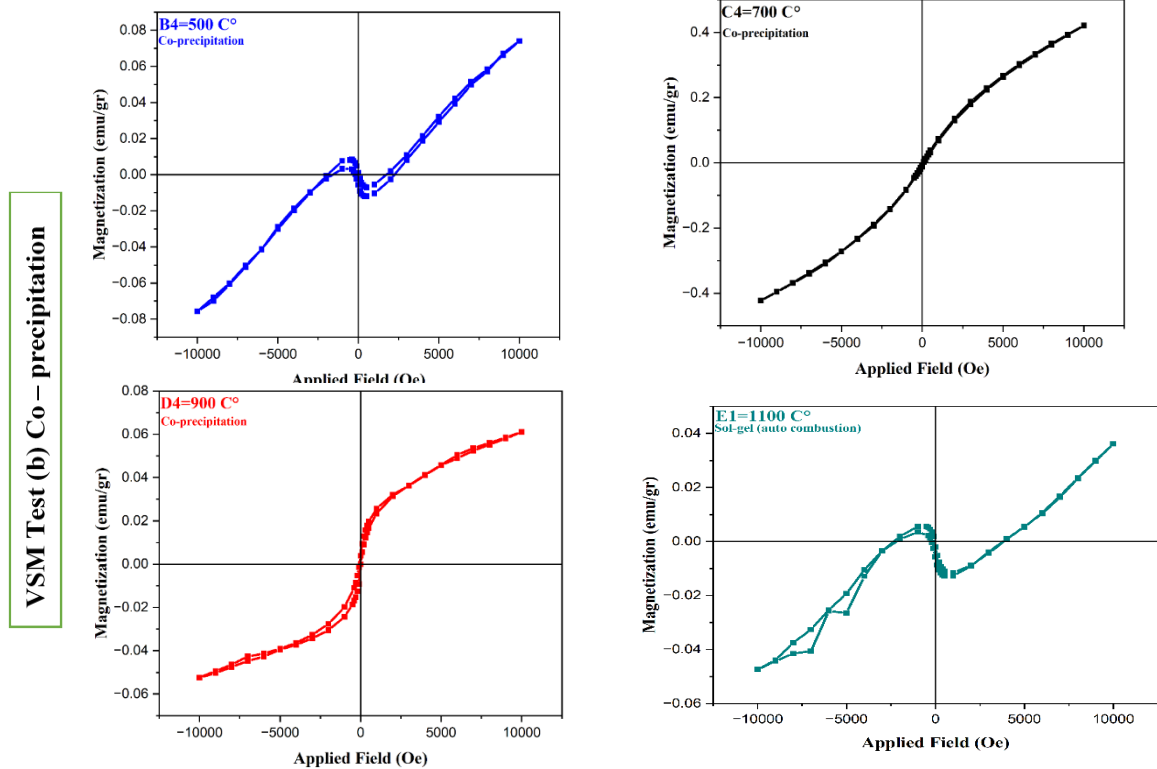
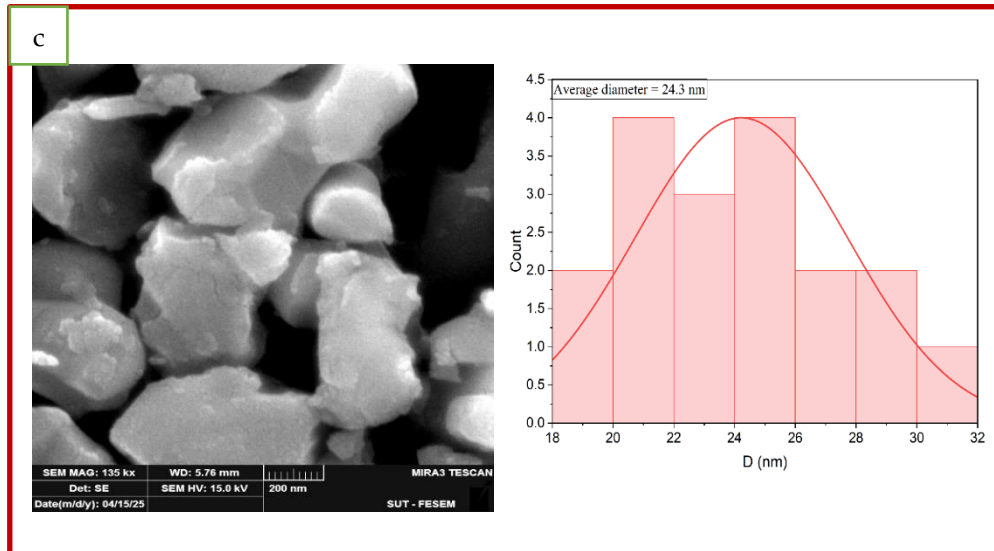
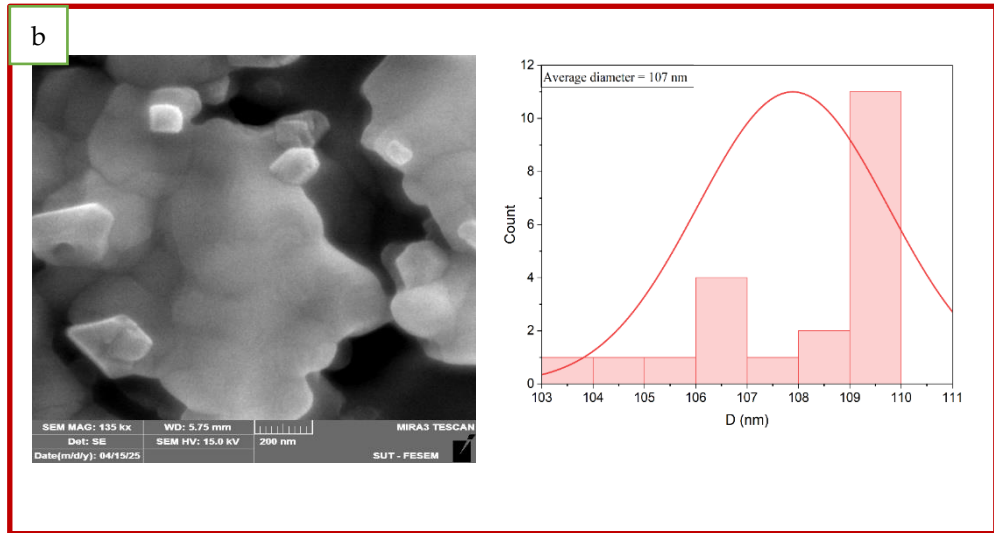
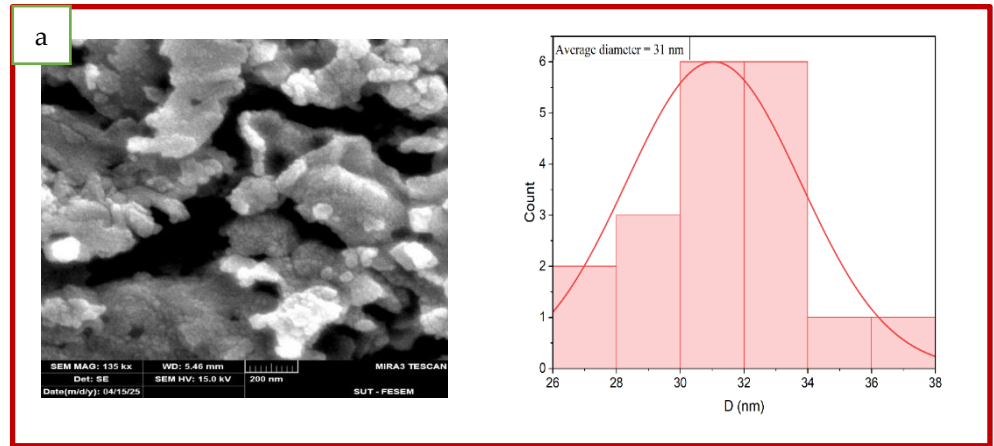


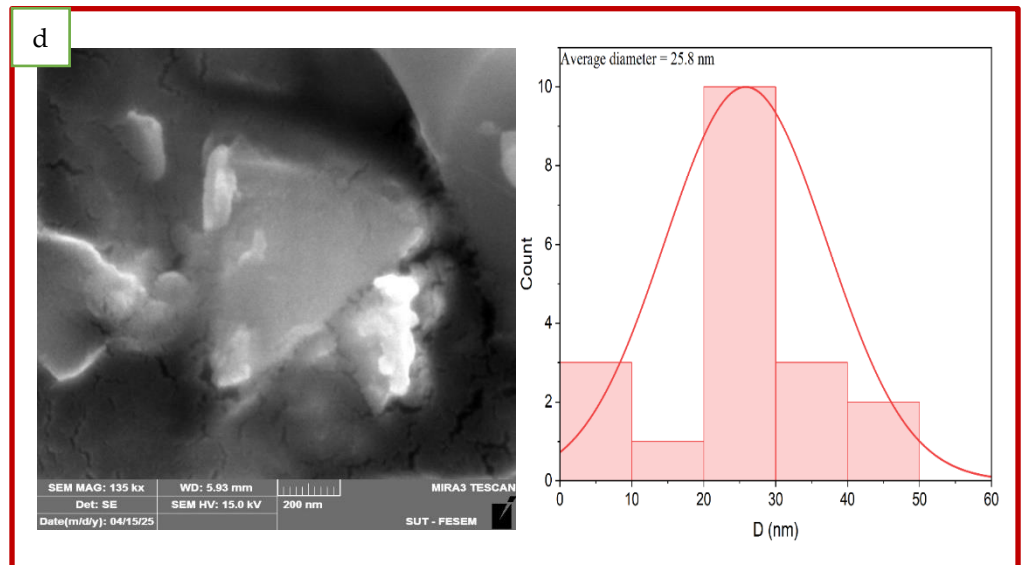
Figure 2. Magnetic hysteresis loop (a) Auto – Combustion (b) Co – precipitation.

FE-SEM Tests

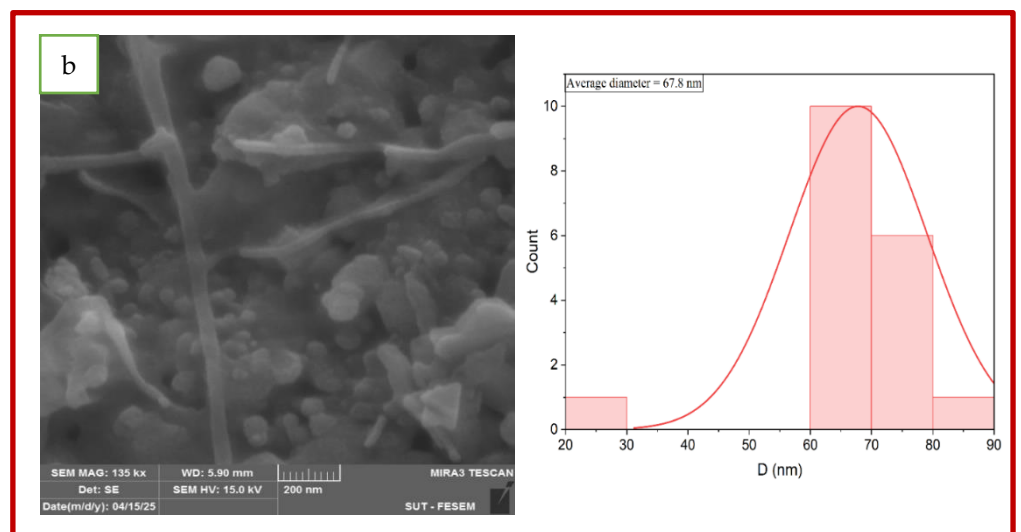
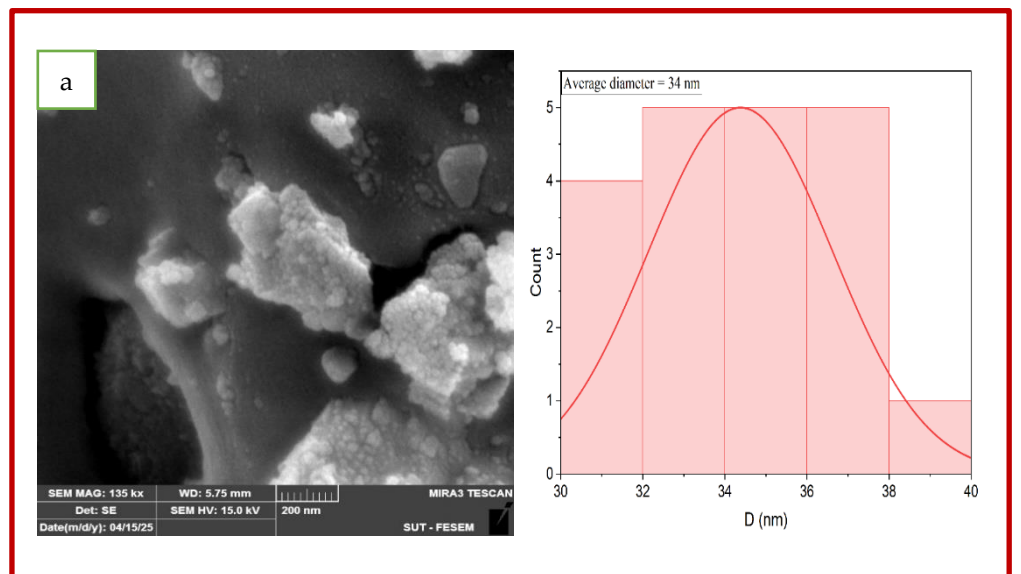
FE-SEM images of the samples prepared by the sol-gel method showed a clear gradient in the evolution of the morphological structure of the particles. At 500 °C, regular nanoparticles with diameters ranging from 24-60 nm were observed, with limited aggregation. As the temperature increases to 900 °C, the grains gradually grow and agglomeration increases, but remains within acceptable limits. At 1100 °C, large particulate agglomerates appear, indicative of crystal fusion and loss of effective nanoscale size. In the co-precipitation method, FE-SEM images show a heterogeneous granular distribution since the lower temperatures. At 500 °C, particles of varying sizes and random aggregates are observed, and stable nanograins are rarely seen. As the temperature rises, the grains increase in size, but show a sharp variation in shape and size, reflecting irregular precipitation reactions. Even at 1100°C, the agglomerates appear irregular and a clear nanostructure is difficult to discern. It can be concluded that the sol-gel method allows finer control over grain growth and shape, producing a material with a more homogeneous grain distribution compared to the co-precipitation method, which suffers from irregular morphology, is shown in Figure 3.

(A)Auto-Combustion





(B) Co-precipitation



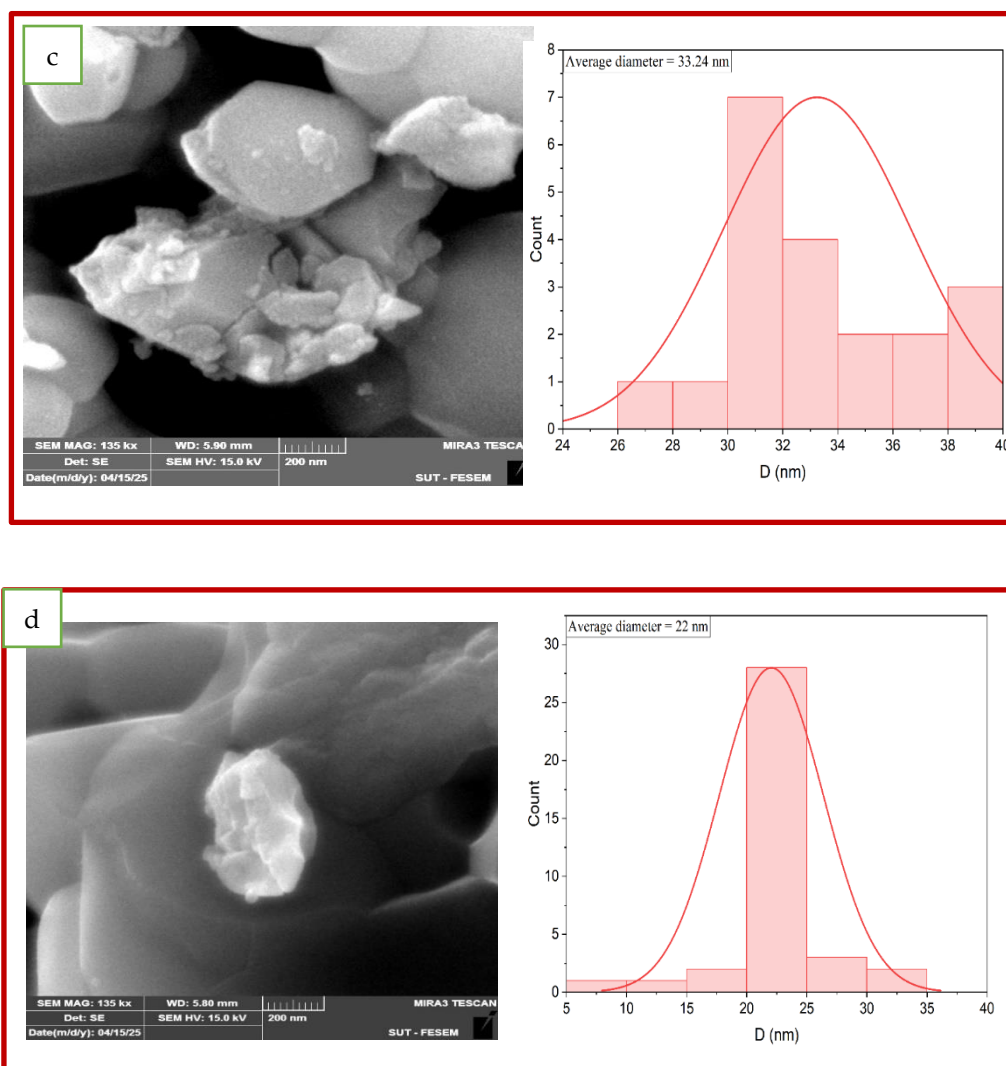
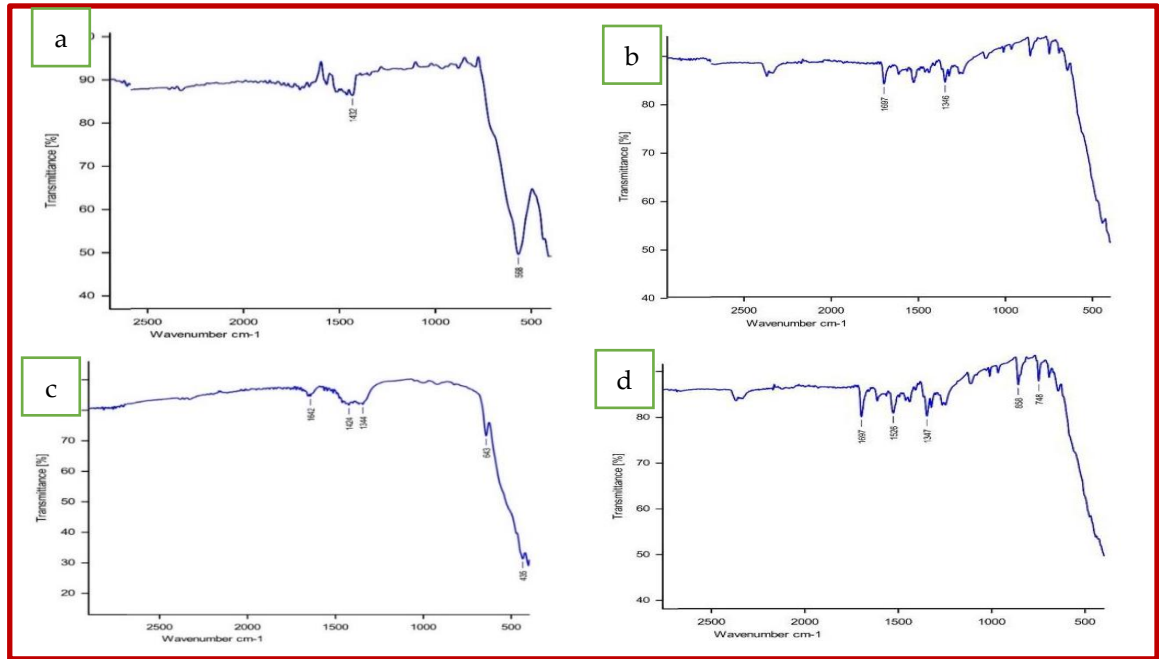


Figure 3. FE-SEM images (A) Auto-Combustion ((a) 500°C ,(b)700°C ,(c) 900°C ,(d) 1100°C), (B) Co-precipitation ((a) 500°C ,(b)700°C ,(c) 900°C ,(d) 1100°C),

FTIR Tests

The The sol-gel spectra showed clear absorption peaks in the 400-600 cm^{-1} bands, which are due to the vibrations of the Fe-O and Ca-O bonds, confirming the beginning of the formation of the $CaFe_2O_4$ spinel network. The peaks were more pronounced at high temperatures, while the organic peaks gradually disappeared, indicating that nitrates and organic compounds were actively decomposed. Secondary peaks were observed at 1600 cm^{-1} and 3500 due to residual moisture, but they weakened with calcination, indicating good degradation of organic compounds, In contrast, the spectra in the co-precipitation method show less sharp peaks at lower temperatures, with peaks associated with organic groups and nitrates remaining visible up to 700°C, Only at 900-1100 °C did the Fe-O and Ca-O peaks start to appear clearly, indicating a slowdown in organic decomposition and crystal lattice formation, these results indicate that Sol-gel spontaneous combustion is more effective in removing organic residues and accelerating crystal lattice formation, while the co-precipitation method requires a longer heat treatment to ensure the purity of the final phase, is shown in Figure 4.

(A) Auto-Combustion



(B) Co-precipitation

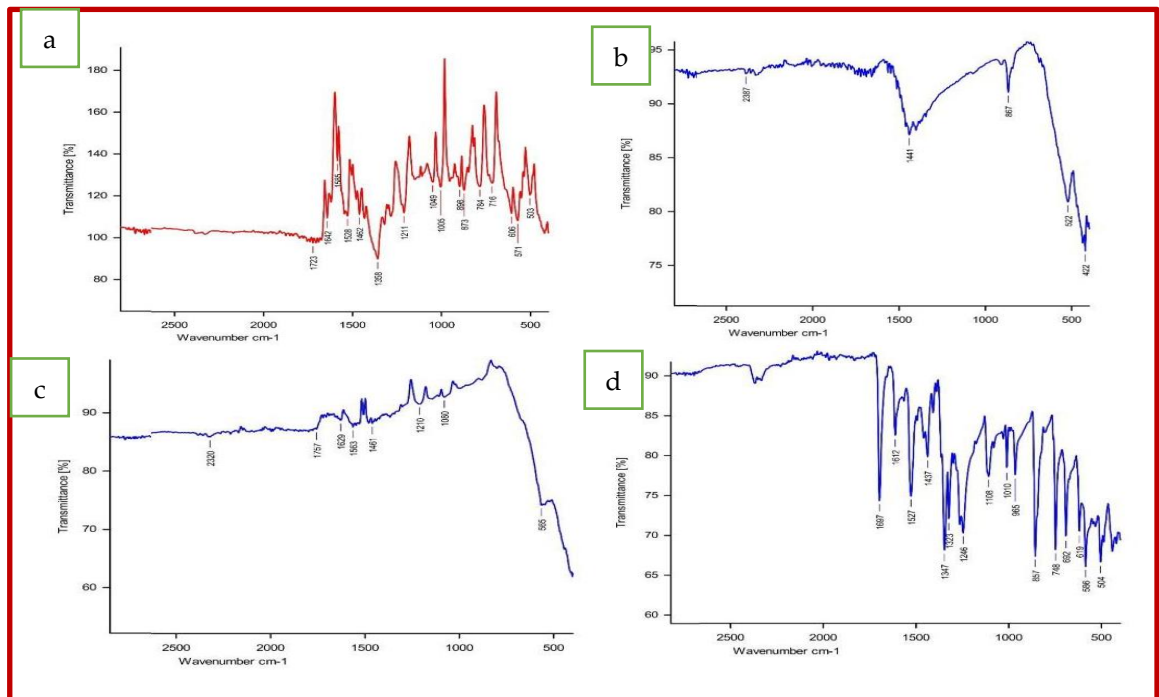
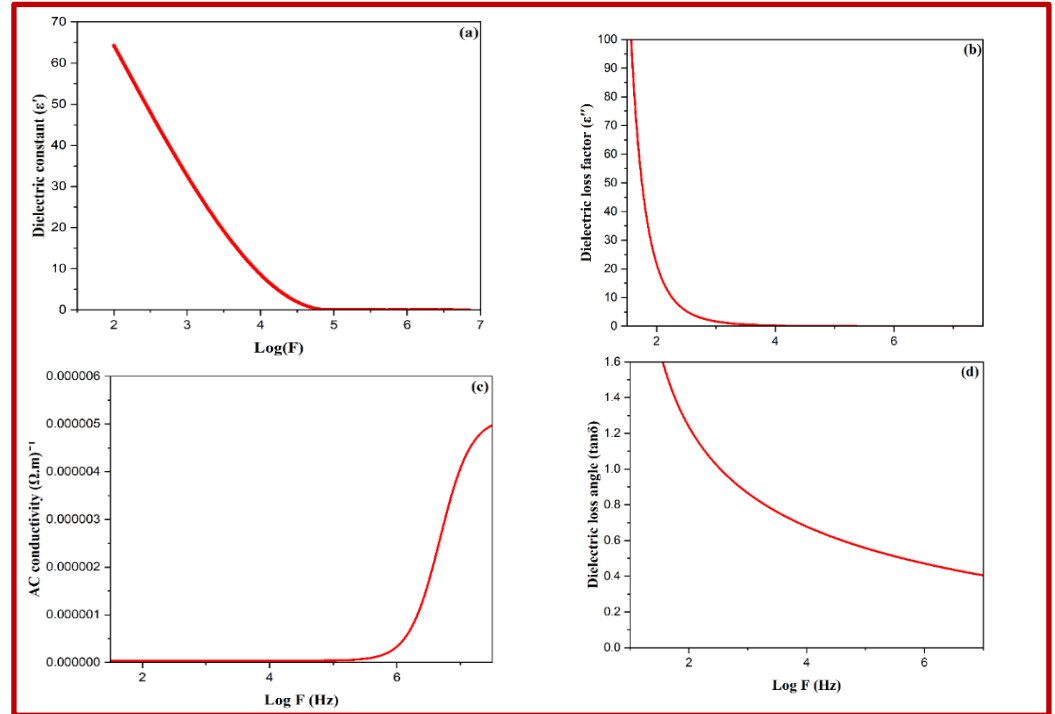


Figure 4. Infrared spectrum (FTIR) (A) Auto-Combustion ((a) 500°C ,(b)700°C ,(c) 900°C ,(d) 1100°C), (B) Co-precipitation ((a) 500°C ,(b)700°C ,(c) 900°C ,(d) 1100°C).

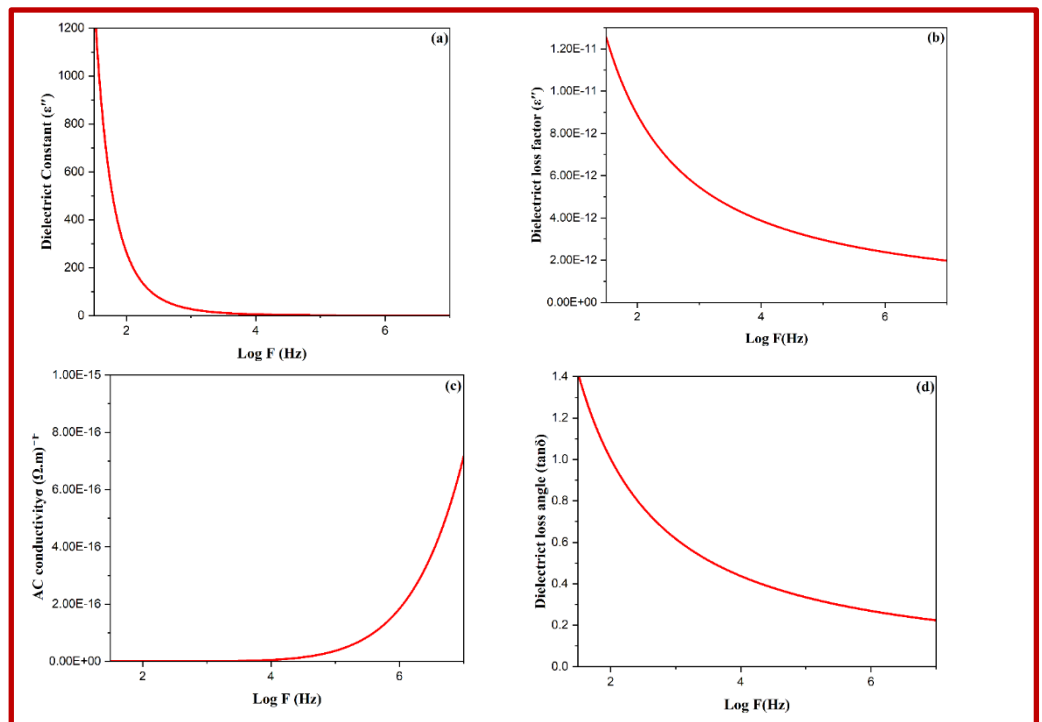
Electrical properties Tests

In terms of electrical properties, the samples prepared by the sol-gel method showed outstanding performance, with the highest value of the true dielectric constant at low frequencies, and a gradual decrease with increasing frequency due to the interfacial polarization response. The AC electrical conductivity showed a markedly increasing pattern at high frequencies, indicating a hopping conduction mechanism. The loss angle $\tan\delta$ decreased with frequency, indicating an improvement in dielectric efficiency at high frequencies. In the co-precipitation method, the samples showed relatively poor electrical properties. The dielectric constant values were significantly lower, and the loss factor

showed irregular behavior, Conductivity was low overall, indicating a heterogeneous structure and obstacles in the movement of charge carriers. The dielectric performance was also unstable at high frequencies, reducing the efficiency of the materials prepared by this method in electronic applications, these data show that the sol-gel method provides materials with improved dielectric properties and electrical conductivity that are suitable for dielectric applications and nanoelectronics components. is shown in Figure 5.



(A)Auto-Combustion



(B) Co-precipitation

Figure 5. Electrical properties (A)Auto-Combustion , (B) Co-precipitation .At 700 Celsius.

4. Conclusion

(CaFe_2O_4) nanoparticles were synthesized via sole-gel auto-combustion and co-precipitation methods to evaluate how synthesis technique influences structural, magnetic, morphological, infrared, and electrical properties. XRD analysis confirmed the formation of orthorhombic structures in both methods, with the sol-gel samples exhibiting sharper diffraction peaks and higher crystallinity, especially at elevated calcination temperatures. Magnetic measurements revealed that sol-gel-derived samples exhibited superior saturation magnetization ($M_s \approx 2.08 \text{ emu/g}$ at 500°C) compared to co-precipitation ($M_s \approx 1.62 \text{ emu/g}$), due to finer particle distribution and better structural homogeneity. FE-SEM images supported these findings, showing more uniform and less agglomerated particles in the sol-gel samples, whereas co-precipitation yielded irregular, clustered morphologies. FTIR spectra demonstrated stronger and more defined metal–oxygen vibrational bands in sol-gel samples, suggesting better decomposition of organic residues. Furthermore, the sol-gel method resulted in higher dielectric constants and AC conductivity, attributed to enhanced grain connectivity and lower porosity. Overall, the sol-gel auto-combustion method provided enhanced control over structural and functional properties, making it more suitable for applications requiring high crystallinity, strong magnetic behavior, and reliable electrical performance. Meanwhile, the co-precipitation method remains a viable low-cost alternative for bulk production with moderate property requirements.

REFERENCES

- [1] M. G. Ibrahim, A. Z. Khalf, and S. M. A. Ridha, "Characterization of Al-Substituted Ni-Zn Ferrites by XRD and FTIR Techniques," 2024.
- [2] R. Taylor *et al.*, "Small particles, big impacts: A review of the diverse applications of nanofluids," *J. Appl. Phys.*, vol. 113, no. 1, 2013.
- [3] S. F. Wang *et al.*, "Highly dispersed spinel (Mg, Ca, Ba)-ferrite nanoparticles: Tuning the particle size and magnetic properties through a modified polyacrylamide gel route," *Ceram. Int.*, vol. 42, no. 16, pp. 19133–19140, 2016.
- [4] T. Zargar and A. Kermanpur, "Effects of hydrothermal process parameters on the physical, magnetic and thermal properties of $\text{Zn}_0.3\text{Fe}_2.7\text{O}_4$ nanoparticles for magnetic hyperthermia applications," *Ceram. Int.*, vol. 43, no. 7, pp. 5794–5804, 2017.
- [5] A. Abedini, A. Rajabi, F. Larki, M. Saraji, and M. S. Islam, "Structural, magnetic and mechanical properties of hydrous Fe/Ni-based oxide components nanoparticles synthesized by radiolytic method," *J. Alloys Compd.*, vol. 711, pp. 190–196, 2017.
- [6] M. Goodarz Naseri, E. B. Saion, and A. Kamali, "An overview on nanocrystalline ZnFe_2O_4 , MnFe_2O_4 , and CoFe_2O_4 synthesized by a thermal treatment method," *Int. Sch. Res. Not.*, vol. 2012, no. 1, p. 604241, 2012.
- [7] S. Ida, K. Yamada, T. Matsunaga, H. Hagiwara, Y. Matsumoto, and T. Ishihara, "Preparation of p-type CaFe_2O_4 photocathodes for producing hydrogen from water," *J. Am. Chem. Soc.*, vol. 132, no. 49, pp. 17343–17345, 2010.
- [8] R. Y. Pawar, "Optimization of reaction conditions in selective oxidation of styrene over fine crystallite spinel-type CaFe_2O_4 complex oxide catalyst," *Mater. Res. Bull.*, vol. 45, no. 5, 2010.
- [9] L. Khanna and N. K. Verma, "Size-dependent magnetic properties of calcium ferrite nanoparticles," *J. Magn. Magn. Mater.*, vol. 336, pp. 1–7, 2013.
- [10] R. A. Candeia, M. I. B. Bernardi, E. Longo, I. M. G. Santos, and A. G. Souza, "Synthesis and characterization of spinel pigment CaFe_2O_4 obtained by the polymeric precursor method," *Mater. Lett.*, vol. 58, no. 5, pp. 569–572, 2004.
- [11] M. Dadwal, D. Solan, and H. Pradesh, "Polymeric nanoparticles as promising novel carriers for drug delivery: an overview," *J. Adv. Pharm. Educ. Res. Jan-Mar*, vol. 4, no. 1, 2014.

- [12] D. Hirabayashi, T. Yoshikawa, K. Mochizuki, K. Suzuki, and Y. Sakai, "Formation of brownmillerite type calcium ferrite ($\text{Ca}_2\text{Fe}_2\text{O}_5$) and catalytic properties in propylene combustion," *Catal. Letters*, vol. 110, pp. 155–160, 2006.
- [13] N. Ikenaga, Y. Ohgaito, and T. Suzuki, "H₂S absorption behavior of calcium ferrite prepared in the presence of coal," *Energy & Fuels*, vol. 19, no. 1, pp. 170–179, 2005.
- [14] M. Arruebo, R. Fernández-Pacheco, M. R. Ibarra, and J. Santamaría, "Magnetic nanoparticles for drug delivery," *Nano Today*, vol. 2, no. 3, pp. 22–32, 2007.
- [15] F. Dumestre, B. Chaudret, C. Amiens, P. Renaud, and P. Fejes, "Superlattices of iron nanocubes synthesized from Fe [N (SiMe₃)₂]₂," *Science (80-.)*, vol. 303, no. 5659, pp. 821–823, 2004.
- [16] S.-J. Park, S. Kim, S. Lee, Z. G. Khim, K. Char, and T. Hyeon, "Synthesis and magnetic studies of uniform iron nanorods and nanospheres," *J. Am. Chem. Soc.*, vol. 122, no. 35, pp. 8581–8582, 2000.
- [17] J. Wan, X. Chen, Z. Wang, X. Yang, and Y. Qian, "A soft-template-assisted hydrothermal approach to single-crystal Fe₃O₄ nanorods," *J. Cryst. Growth*, vol. 276, no. 3–4, pp. 571–576, 2005.
- [18] Z. Yuanbi and Q. I. U. Zumin, "Preparation and analysis of Fe₃O₄ magnetic nanoparticles used as targeted-drug carriers," *Chinese J. Chem. Eng.*, vol. 16, no. 3, pp. 451–455, 2008.
- [19] M. Faraji, Y. Yamini, and Mjj. Rezaee, "Magnetic nanoparticles: synthesis, stabilization, functionalization, characterization, and applications," *J. Iran. Chem. Soc.*, vol. 7, pp. 1–37, 2010.
- [20] E. Ruiz-Hernández, A. Lopez-Noriega, D. Arcos, I. Izquierdo-Barba, O. Terasaki, and M. Vallet-Regí, "Aerosol-assisted synthesis of magnetic mesoporous silica spheres for drug targeting," *Chem. Mater.*, vol. 19, no. 14, pp. 3455–3463, 2007.
- [21] S. M. A. Ridha and M. A. Awad, "Structural characteristics of M-type Ba-Sr hexaferrite nanoparticles prepared using sol-gel method: role of the Sr-ion concentrations and annealing temperatures," *Turkish J. Comput. Math. Educ.*, vol. 12, no. 14, pp. 663–674, 2021.